ISSN 1068-3356, Bulletin of the Lebedev Physics Institute, 2010, Vol. 37, No. 6, pp. 184–190. © Allerton Press, Inc., 2010.
Original Russian Text © S.V. Borisov, M. Boezio, S.A. Voronov, A.M. Galper, G. Jerse, A.V. Karelin, E. Mocchiutti, P. Picozza, O. Adriani, G.A. Bazilevskaya, R. Bellotti, V. Bonvicini, L. Bonechi, S. Bottai, A. Bruno, A. Vacchi, E. Vannuccini, G. Vasil'ev, J. Wu, L. Grishantseva, M.P. De Pascale, C. De Santis, N. De Simone, V. Di Felice, W. Gillard, G. Zampa, N. Zampa, V.G. Zverev, M. Casolino, D. Campana, R. Carbone, G. Castellini, P. Carlson, F. Cafagna, A.N. Kvashnin, S.V. Koldashov, L. Consiglio, S.Yu. Krutkov, A. Leonov, V. Malvezzi, L. Marcelli, W. Menn, V.V. Mikhailov, A. Monaco, N. Mori, N. Nikonov, G. Osteria, P. Papini, M. Pearce, S.B. Ricciarini, M. Ricci, L. Rossetto, M. Simon, R. Sparvoli, P. Spillantini, Yu.I. Stozhkov, P. Hofverberg, Yu.T. Yurkin , 2010, published in Kratkie Soobshcheniya po Fizike, 2010, Vol. 37, No. 6, pp. 35–45.

Measurement of the High-Energy Electron and Positron Spectrum in the PAMELA Experiment

S. V. Borisov, M. Boezio, S. A. Voronov, A. M. Galper, G. Jerse, A. V. Karelin, E. Mocchiutti, P. Picozza, O. Adriani, G. A. Bazilevskaya, R. Bellotti, V. Bonvicini, L. Bonechi, S. Bottai, A. Bruno, A. Vacchi, E. Vannuccini, G. Vasil'ev, J. Wu, L. Grishantseva, M. P. De Pascale, C. De Santis, N. De Simone, V. Di Felice, W. Gillard, G. Zampa, N. Zampa, V. G. Zverev, M. Casolino, D. Campana, R. Carbone, G. Castellini, P. Carlson, F. Cafagna, A. N. Kvashnin, S. V. Koldashov, L. Consiglio, S. Yu. Krutkov, A. Leonov, V. Malvezzi, L. Marcelli, W. Menn, V. V. Mikhailov, A. Monaco, N. Mori, N. Nikonov, G. Osteria, P. Papini, M. Pearce, S. B. Ricciarini, M. Ricci, L. Rossetto, M. Simon, R. Sparvoli, P. Spillantini, Yu. I. Stozhkov, P. Hofverberg, and Yu. T. Yurkin

Received April 6, 2010

Abstract—The PAMELA magnetic spectrometer onboard the Resurs DK1 satellite no. 1 was put into (Earth) orbit on June 15, 2006; measurements continue at the present time. The scientific objective of the spectrometer is the study of antiproton, proton, positron, electron and light nucleus fluxes in cosmic rays. In this paper, we present the technique for measuring electron and positron spectra in the energy range from 20 to 800 GeV.

DOI: 10.3103/S1068335610060096

Key words: PAMELA magnetic spectrometer, cosmic rays, high-energy positrons and electrons.

1. The PAMELA magnetic spectrometer is intended to perform precision measurements of antiproton, positron, and electron spectra to energies of the order of several TeV and to search for light antinuclei.

The device consists of the following detectors (Fig. 1, top-down): time-of-flight system TOF (S1, S2, S3), magnetic spectrometer, anticoincidence system (CARD, CAT, CAS), electromagnetic calorimeter, shower detector (S4), and neutron detector. The time-of-flight system consisting of three double layers of scintillation bars is intended to measure the incident particle ionization, time and direction of its flight in the device. The magnetic spectrometer consists of six layers of silicon microstrip detectors placed into a magnetic field and measures the coordinate of the detector plane intersection by a particle in both X and Y projections. In measuring the particle trajectory curvature in the magnetic field, the particle rigidity (the momentum-to-charge ratio) is reconstructed. The anticoincidence system rejects the events occurred outside the device aperture. The electromagnetic position-sensitive calorimeter is an assembly of 22 tungsten planes of equal thickness, sandwiched by silicon strip detectors whose strips are arranged with a step of 2.4 mm; in any two neighboring planes, they are mutually perpendicular, which makes it possible to reconstruct the three-dimensional pattern of the particle interaction with calorimeter material. The full thickness of the calorimeter is 16.3 radiation lengths and 0.6 of nuclear interaction length. The shower detector is a scintillator viewed by six photomultipliers (PMs); it measures the energy leakage from the calorimeter. The neutron detector is intended to detect neutrons produced at the particle interaction in the calorimeter, which makes it possible to improve hadron and lepton separation. The geometrical factor of the PAMELA device is 21.6 cm^2sr.

The entire PAMELA device, its individual detectors, and measurement conditions are described in more detail in [1].

2. Problem statement and the calorimeter of the PAMELA spectrometer. Of particular interest for measurements in the energy region above 100 GeV is the cosmic-ray electron component, since, as is assumed, annihilation of dark matter particles or such astrophysical objects as pulsars and supernova

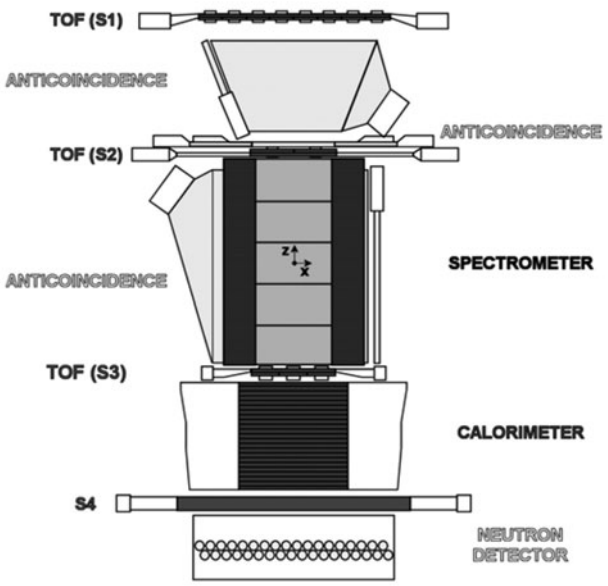

Fig. 1. Structure of the PAMELA magnetic spectrometer (see text for details).

explosions can contribute to the electron and positron spectrum. However, the measurement of the electron spectrum in this region seems to be a rather difficult problem. Such measurements using ground-based setups for measuring extensive air showers are impossible, since it is impossible to separate electron events against the background of proton events. The measurements onboard high-altitude balloons at 30–40 km over the Earth's surface are complicated by the residual atmosphere, particle interactions with which distort the measured spectrum. Thus, it is best to measure the high-energy electron component of cosmic rays in near-Earth space.

Currently, such measurements are performed by two devices, i.e., the PAMELA spectrometer and FERMI gamma telescope. Among the advantages of the PAMELA device is the thick calorimeter (16.3 radiation lengths X_0 in comparison with $8.6X_0$ of the FERMI calorimeter), which allows the PAMELA calorimeter to measure the incident electron energy with an accuracy of $\sim$10% up to several TeV.

In the PAMELA spectrometer, the electron and other components of cosmic rays are measured in the energy range from hundreds MeV to 200–300 GeV using a magnetic track system which provides reliable measurements of particle momenta to several hundred GeV (the maximum measured rigidity is 740 GeV/s) [2]. However, to study the spectrum in the region above several hundred GeV, only a calorimeter can be used [3].

3. Technique for identifying high-energy electrons and their spectrum measurement. The developed method makes it possible to identify electrons and positrons against the background of protons and to measure their energy in the range from $\sim$20 GeV to several TeV. The technique was developed based on Monte Carlo calculations using the GPAMELA official simulation package of the PAMELA collaboration [4], which reproduces the complete spectrometer geometry and is based on the GEANT3 physical simulation package and the GHEISHA package for simulating hadron interactions.

The calorimeter is sufficiently thick that all electrons with energies above 20 GeV could develop a shower in it; thus, only events causing a cascade in the calorimeter should be considered in the subsequent analysis.

The total energy release and the number of triggered strips in the electromagnetic shower is correlated with the primary electron energy; therefore, having imposed constraints on these values, it is possible to reject most noninteracting particles or showers initiated deep in the calorimeter, which are identified as proton events. Then, to separate electrons in remained showers, it is required to reconstruct the cascade axis to reject particles arrived outside the spectrometer aperture, and to calculate the topological parameters of analyzed showers in the calorimeter. The axis is reconstructed using the multi-iteration least squares method over centroids of energy releases in planes. The angular resolution improves with the primary particle energy; at several hundred GeV, it is of the order of several thousandths of radian.

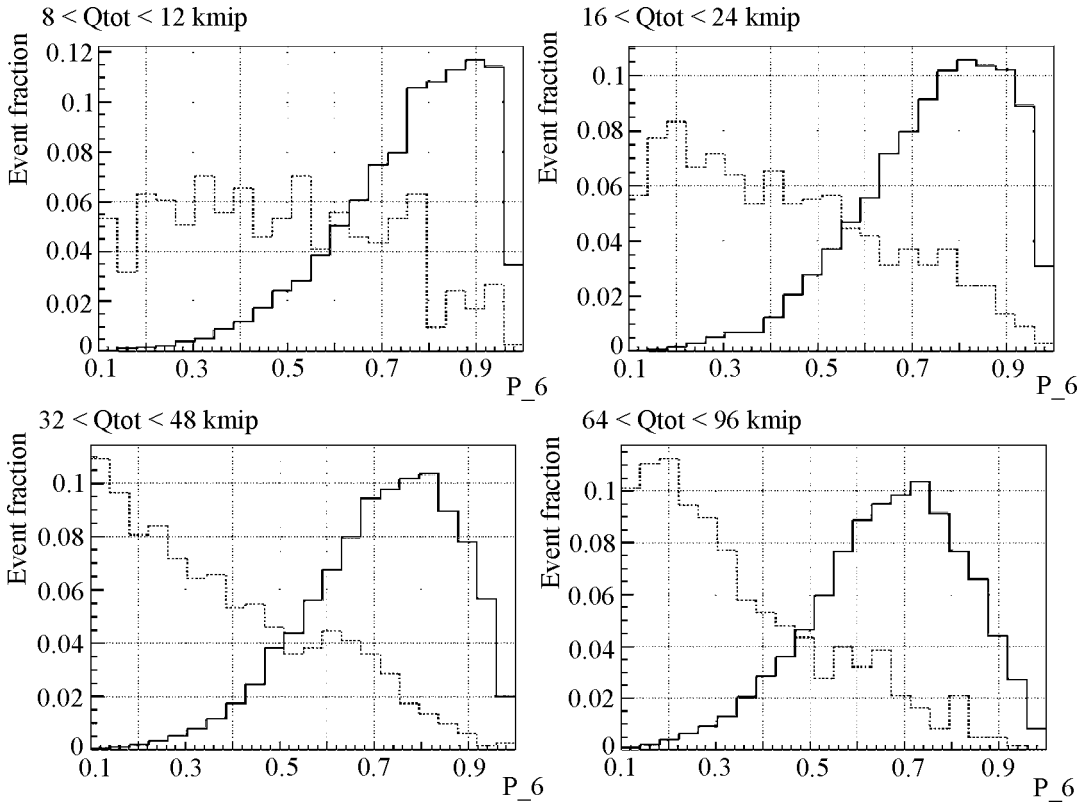

Fig. 2. Electron and proton distributions over the energy release fraction for various ranges of total energy releases (see text for details).

But even at relatively low energies (of the order of tens of GeV), it is about one hundredth of radian. For further analysis, only those showers are retained, whose extrapolated axis has passed at a certain distance from magnet walls, which is determined by angular resolution for each particular event.

Then, since electromagnetic cascades are more regular than hadron ones, the shower axis reconstruction accuracy is, correspondingly, better in the former case. This leads to smaller values of χ^2 of the axis approximation, which allows proton suppression at this selection stage.

As the cascade axis is reconstructed, the parameters characterizing the shower development can be calculated. The separation of hadron and electromagnetic cascades is based on the parameters describing in detail the shower development in the first four layers of the calorimeter. These parameters are the number of triggered strips, the energy release after a given tungsten absorber layer, the cascade growth from layer to layer, the energy release fraction in the cylinder 1 strip in radius in the cluster of triggered strips on the reconstructed shower axis. As an example, Fig. 2 shows the electron and proton distribution over the energy release fraction within a radius of one strip from the shower axis after the first tungsten layer for various ranges of total energy releases in the calorimeter (denoted by Q_{tot} above each of four diagrams; the range is given in thousands of MIPs; in the case of an electron shower, one thousand of MIPs approximately corresponds to the primary particle energy of 5 GeV). This parameter is the horizontal axis; the vertical axis is the fraction of events from a given range. Black solid and grey dashed curves are the distributions for electrons and protons, respectively. This criterion rejects approximately half the hadron showers in the entire energy range of interest; in this case, 2–4% of electrons are lost.

To suppress the nuclear component of cosmic rays, the criteria related to the shower development, damping, and homogeneity are used, which makes it possible to reduce the proton contribution to a level of ~5–10% of the measured electron flux. The calculations also showed that the electron selection efficiency is ~50–60% almost in the whole energy range. A certain decrease in the efficiency to 25–30% at energies of the order of several tens of GeV is caused by the use of a narrower aperture for event

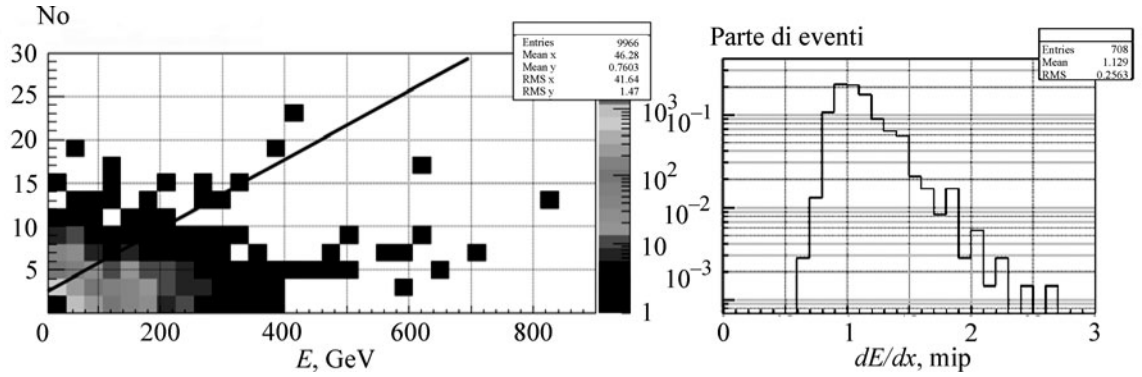

Fig. 3. (a) Distribution of electrons selected using the calorimetric technique (see text for details); (b) Distribution of events over the average energy loss dE/dx for an energy range from 37 to 50 GeV.

selection, controlled by spatial resolution in each particular case. In the case of a cascade caused by an electron or a positron with an energy of the order of several tens of GeV, the resolution appears such that the narrowed aperture appears about twice smaller than the nominal one. At energies above 100 GeV, statistics loss due to the narrowed aperture instead of the nominal one is only 10%.

The electron energy is measured by the total energy release in the calorimeter. The resolution of such an energy measurement method is less than 10%. If the shower completely fits into the calorimeter, the dependence between the total energy released in the cascade and the primary energy is linear; however, if a shower fraction falls outside the physical volume of the calorimeter, it is necessary to introduce a nonlinear correction. It was found that it is sufficient to use the second-degree polynomial in the energy range of our interest, exactly what was done.

After completing the selection over the shower pattern, selection over the number of neutrons per event is applied. This criterion is based on that the development of the hadron cascade is, as a rule, associated with the interaction with calorimeter material nuclei, which is accompanied by emission of a large number of neutrons. In the case of the electromagnetic shower, neutrons can be produced only due to photonuclear reactions. As a result, the probability of detection of a large number of neutrons in the hadron shower is appreciably higher than in the electromagnetic shower. A quantitative criterion was developed as follows. Using magnetic analysis, electrons up to an energy of 180 GeV were selected in the flight data of the PAMELA spectrometer. We note that the combined use of the magnetic spectrometer and calorimeter allows very reliable selection of electrons, since the flux of hadron particles with negative charge (only antiprotons) is two orders of magnitude smaller than the electron flux; thus, such a simple criterion as the comparison of energies measured using the magnetic spectrometer and calorimeter allows suppression of the hadron component by a factor of more than 10^4 [3]. For electrons selected in such a way the distributions over the number of neutrons were constructed for different energy ranges. Based on the analysis of the distributions, the selection criterion was developed, which allows retention of 99.5% of electron events. The maximum allowed number of neutrons per event is defined as a function of energy, $N_{\max} = 2 + 0.04 \cdot E$, where E is the energy in GeV. Figure 3(a) shows the distribution of electrons selected using the calorimetric technique in the experimental data of the PAMELA spectrometer by the number of neutrons and the energy (the vertical axis is the number of neutrons per event, the horizontal axis is the energy in GeV). The straight line in the diagram is the threshold number of neutrons. According to this threshold, 3% of events selected using the calorimeter were rejected.

Selection over the ionization loss in scintillators of the time-of-flight system was also performed. Since cosmic rays, in addition to protons, contain a significant fraction of nuclei (to 10%), to eliminate the need for the analysis of their suppression by the criteria over the calorimeter and neutron detector, an additional criterion was introduced, developed based on experimental data of the spectrometer on specific ionization losses (dE/dx) in scintillation detectors.

To increase the criterion efficiency, events were selected by the "truncated mean" of measurements in S1 and S2. The data of S3 were not used due to the possible effect of the reverse current of cascades at high energies. To calculate the truncated mean, the following algorithm was used.

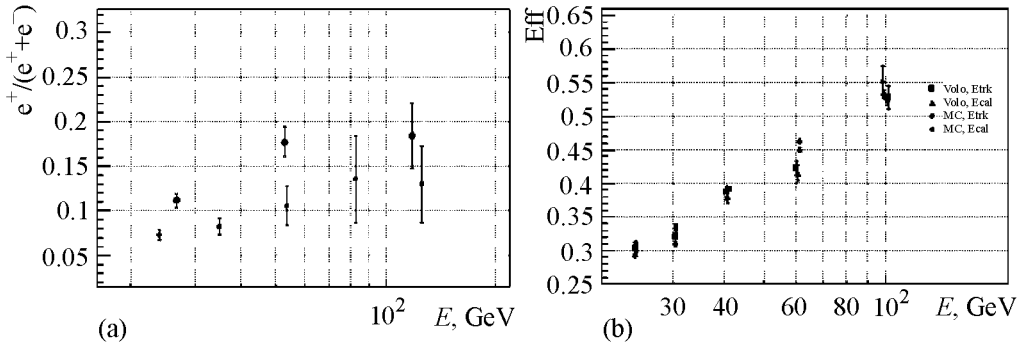

Fig. 4. (a) Estimate of the residual proton contamination. Small circles correspond to the positron fraction [5]; larger circles are charge ratios; (b) the efficiency of event selection by the spectrometer (squares) and calorimeter (triangles), and corresponding model data (open and closed circles).

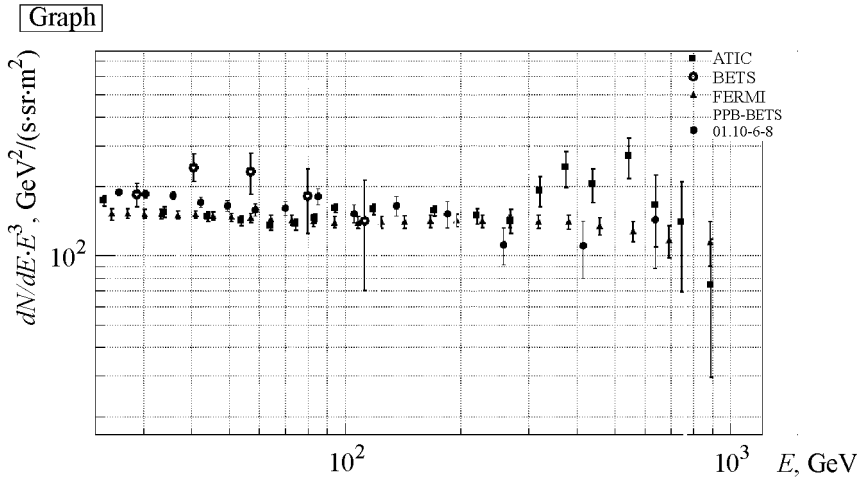

Fig. 5. Spectra measured in different experiments: the values obtained using the presented technique (large closed circles), the values for electrons measured in the ATIC experiment [6] (closed squares), in the BETS experiment [7] (dark gray open circles), PPB-BETS experiment [8] (light gray open triangles), FERMI experiment [9] (dark gray triangles).

(i) The average M of measurements in four scintillators arranged above the magnetic track system is calculated.

(ii) The measured values twice larger than the average M are rejected, and a new average $M1$ is calculated.

(iii) The measured values ten times lower than the average $M1$ are rejected, and a new average $M2$ is calculated.

The distribution of events over the average energy loss dE/dx for the energy range from 37 to 50 GeV, calculated in such a way, is shown in Fig. 3(b). The dependence of the particle selection efficiency on the thresholds was studied. The efficiencies of selection over upper and lower boundaries were studied separately. Based on the analysis performed, the optimum electron selection range was determined as 0.5–2.3 MIP. The electron selection efficiency using this criterion was more than 99% independently of energy.

This criterion was applied to events selected using the calorimeter and neutron detector. A total of 4% of events were rejected.

4. Technique testing. To achieve reliable measurements of spectra, the developed technique was comprehensively tested, i.e., residual hadron contamination was estimated using magnetic analysis in

the energy range to 150 GeV, the efficiency was estimated by experimental data, and the time stability of detectors was tested.

The residual proton contamination was estimated as follows. Among the events selected using the described technique, particles with reliably approximated trajectories in the magnetic spectrometer were selected. For such events, the fraction of positive particles was calculated. An excess of this fraction for events selected using the described technique over the actual positron fraction yields the estimate of the proton contamination. The result of such estimation is shown in Fig. 4(a): small circles correspond to the positron fraction according to [5], large circles are charge ratios for analyzed events. Thus, the analysis of the magnetic spectrometer data shows that the contribution of protons to the electron and positron spectrum is about a few percent, and the contamination value does not increase with energy.

Another important characteristic of the technique is the event selection efficiency. The accuracy of its calculation based on the Monte Carlo method was tested using magnetic analysis in the energy range to 150 GeV. This was done as follows: the criteria of the technique described above were applied to electrons separated in flight data based on magnetic analysis, and the fraction of electrons selected for different energy ranges was calculated. The energy was measured by the calorimeter and magnetic spectrometer. A similar procedure was performed in model data. The result of comparison of such an estimate based on experimental and model data is shown in Fig. 4(b). Squares and triangles are the efficiency estimates by flight data with energy measurements by the magnetic spectrometer and calorimeter, respectively. Open and closed circles correspond to a similar estimate from model data. We can see that the experimental and simulation data show very good agreement.

Finally, the measured flux stability was tested. The time stability of the total flux at high energies will mean detector operation stability, since the flux temporal variation, if exists, has a negligible value at high energies (above 20 GeV), as follows from the analysis of experimental data.

To obtain such an estimate, the entire measurement period ($\sim$30 months) was divided into intervals about two months long; for each interval, the total electron and positron flux was calculated. The result of this estimation showed that the flux remain constant within the statistical error, which indicates the spectrometer operation stability.

5. Results and discussion. After comprehensive tests of the technique by the experimental data of the PAMELA spectrometer for 2.5 years of measurements, the total electron–positron spectrum was constructed in the energy range from 24 to 800 GeV. The spectrum is close to the power-law one with an exponent of -3.15 ± 0.04 and has a feature at energies of 70–200 GeV.

The spectrum measured using the described technique was also compared with the electron spectra measured using the techniques based on magnetic analysis. The comparison showed that the spectra measured by different methods coincide within the error.

The measured spectrum coincides with the results of previous experiments in both magnitude and the exponent (-3.15) averaged over the whole range with the results of previous experiments of previous experiments (see Fig. 5; which shows the values obtained using the presented technique (large closed circles), the values for electrons measured in the ATIC experiment [6] (closed squares), in the BETS experiment [7] (dark gray open circles), PPB-BETS experiment [8] (light gray open triangles), FERMI experiment [9] (dark gray triangles)).

6. Conclusions. The described method allows efficient selection of high-energy electrons to $\sim$1 TeV; the contribution of protons is a few percent. The performed tests confirmed the technique accuracy. The total electron and positron spectrum in the energy range of from 24 to 800 GeV was obtained; the spectrum is power-law with an average exponent of -3.15 ± 0.04; the flux magnitude is in agreement with to the results of previous experiments.

ACKNOWLEDGMENTS

This study was supported in part by the Russian Foundation for Basic Research, project no. 07-02-000922a.

The authors are grateful to the Research Center for Earth Operative Monitoring and the State Research and Production Space-Rocket Center "TsSKB-Progress" for their assistance in the experiment performance.

REFERENCES

1. P. Picozza et al., Astropart. Phys. **27**, 296 (2007).
2. S. Straulino, et al., Nucl. Instrum. Methods A **530**, 168 (2004).
3. S. V. Borisov, S. A. Voronov, and A. V. Karelin, Usp. Fiz. Nauk **179**, 931 (2009).
4. A. Bruno, PhD Thesis (Universita degli Studi di Bari, Bari, Italy, 2009).
5. O. Adriani et al., Nature **458**, 607 (2009).
6. J. Chang et al., Nature **456**, 362 (2008).
7. S. Torii et al., Astropart. Phys. **559**, 973 (2001).
8. S. Torii et al., Adv. Polar Upper Atm. Res. **20**, 52 (2006).
9. A. A. Abdo et al., Phys. Rev. Lett. **102**, 181101 (2009).